Nigerian Journal of Technology (NIJOTECH)
Vol. 43, No. 4, December, 2024, pp.666 - 675
www.nijotech.com

Print ISSN: 0331-8443
Electronic ISSN: 2467-8821
https://doi.org/10.4314/njt.v43i4.7

COMPREHENSIVE STUDY OF EXTRACTION AND APPLICABILITY OF NANOSILICATE PARTICLES FROM NATURAL WASTE FOR BIOPOLYMER REINFORCEMENT

AUTHORS:
H. O. Onovo[1,*], A. A. Agbeleye[2], T. T. Akano[3], D. B. Oludele[4], J. O. Olawoyin[5], and I. S. Kentosu[6]

AFFILIATIONS:
[1,2,4,5,6]Department of Metallurgical and Materials Engineering, Faculty of Engineering, University of Lagos, Lagos State. Nigeria.
[3]Department of Mechanical Engineering, University of Botswana Gaborone, Botswana

***CORRESPONDING AUTHOR:**
Email: honovo@unilag.edu.ng

ARTICLE HISTORY:
Received: 16 January, 2024.
Revised: 04 November, 2024.
Accepted: 28 November, 2024.
Published: 31 December, 2024.

KEYWORDS:
Biodegradability, Renewability, Biopolymers, Nano-silica, Corncob, Environmental sustainability, Natural waste, Polymer degradation.

ARTICLE INCLUDES:
Peer review

DATA AVAILABILITY:
On request from author(s)

EDITORS:
Ozoemena Anthony Ani
Patrick Akpan

FUNDING:
None

Abstract

Biopolymers have emerged as a promising alternative to traditional petroleum-based plastics owing to their inherent biodegradability and renewability. However, augmenting their mechanical and barrier properties remains pivotal for diverse applications, particularly in packaging applications. This study explores corncob nano-silica (ccnSi) extraction, evaluating its performance in biopolymer films. A synergistic chemical-mechanical process yielded uniformly sized ccnSi particles (69.23-97.70 nm). To optimize ccnSi incorporation, surface treatments with varying NaOH concentrations (3.0M, 3.5M, 4.0M) were applied. The extracted ccnSi's performance metrics rivaled commercial nano-silica (cnSi). X-ray fluorescence (XRF) analysis unveiled a heightened silicon content in ccnSi (94 %) relative to cnSi (71.61 %). Scanning electron microscopy (SEM) and Energy dispersive X-ray (EDX) analyses substantiated the commendable dispersion and amorphous characteristics of the ccnSi/biopolymer composites. Using Fourier transform infrared spectroscopy (FT-IR) provided empirical evidence for the existence of groups of silanol as well as the silane, signifying surface modifications. Substantial surface areas (324.9-833.6 m^2/g) were ascertained through Brunauer-Emmett-Teller (BET) analysis, a finding further affirmed through the dynamic light scattering (DLS) and particle size distribution (PSD) measurements. The incorporation of ccnSi markedly elevated the tensile strength of biopolymer films (0.572 MPa) in contrast to cnSi (0.49 MPa). Thermogravimetric and Differential thermal analysis (TGA-DTA) indicated commendable thermal stability, with polymer degradation initiating at 400 °C. The glass transition temperature (Tg) of 32 °C, coupled with the amorphous nature confirmed by Differential scanning calorimetry (DSC), underscores the promising potential of ccnSi as a biopolymer. This research underscores the successful extraction and application of ccnSi in biopolymer-based films, presenting a paradigm shift towards enhanced performance and heightened environmental sustainability in next-generation packaging materials.

1.0 INTRODUCTION

Motivated by an escalating concern for environmental issues, the agricultural sector has garnered significant attention as a critical domain for addressing agro-waste and fostering sustainable practices [1, 2]. In response to this imperative, the emergence of nanotechnology has presented a transformative avenue, allowing for the repurposing of agricultural waste into reusable raw materials and the synthesis of versatile nanomaterials [3, 4]. Silica nanoparticles (SiNPs), in particular, have garnered significant attention in this context, particularly due to their versatile applications in the biomedical field [5, 6].

HOW TO CITE:
Onovo, H. O., Agbeleye, A. A., Akano, T. T., Oludele, D. B., Olawoyin, J. O., and Kentosu, I. S. "Comprehensive Study of Extraction and Applicability of Nanosilicate Particles from Natural Waste for Biopolymer Reinforcement", *Nigerian Journal of Technology*, 2024; 43(4), pp. 666 – 675; *https://doi.org/10.4314/njt.v43i4.7*

The agricultural industry, characterized by the generation of copious amounts of waste, is witnessing a paradigm shift towards harnessing agricultural residues such as crop leftovers for the production of value-added products, including nanoparticles [7, 8]. Among these residues, corn cobs (CC), ubiquitous agricultural byproducts, represent a significant opportunity for resource utilization [9]. Despite their intrinsic value and the myriad potential applications associated with them, corn cobs, notably in the domain of biopolymer reinforcement, continue to be largely underutilized [10]. Traditional agricultural waste management practices, often entailing the indiscriminate discarding of corn cobs, contribute to environmental concerns and inefficiencies in resource utilization [11]. Notably, this underutilized agricultural material holds immense promise owing to its abundance and inherent silica content [9]. Concurrently, biopolymers are emerging as a sustainable alternative to conventional plastics, primarily due to their eco-friendly profile [12, 13]. However, the broader industrial adoption of biopolymers is contingent upon advancements in their mechanical and barrier properties [14, 15].

This research endeavors to bridge existing knowledge gaps by concentrating on the extraction of nano silica from corn cobs through a precipitation method, drawing inspiration from established protocols [16, 17]. Subsequently, the extracted SiNPs are incorporated into biopolymer films to evaluate their efficacy in enhancing various properties, building upon and extending prior research in the area of biodegradable materials [18, 19]. The importance of this study resides in its potential to unlock the hitherto untapped potential of corn cobs and substantially contribute to the development of sustainable materials, thus aligning with broader goals of waste minimization and adherence to circular economy principles [20, 21].

2.0 MATERIALS AND METHODS

2.1 Materials

The materials employed in this study consist of raw corn cob procured locally. In addition, all relevant chemicals, including sodium hydroxide pellets (NaOH), and concentrated acids such as sulfuric (H_2SO_4), hydrochloric (HCl), and ammonia (NH_3), were utilized. Furthermore, all chemicals made use of in the course of this experiment conformed to analytical grade, and hence, there was no need for further purification before use. The apparatus and equipment utilized in the experimental procedures include 100 ml, 250 ml, and 400 ml beakers, sample bottles, racks, a magnetic stirrer, a hot plate, a Kjeldahl digester, digestion tubes, a retort stand, an analytical balance, an oven, filter paper, a reflux condenser, a fume cupboard, and a watch glass.

2.2 Preparation of Corncob Ash (CCA) Precursor for Nano-Silica Extraction

The corn cobs underwent a thorough cleansing process with distilled water (performed three times) to eliminate dust and potential contamination. Subsequently, the cobs were sectioned into pieces and left to sun-dry for a week, after which the samples were subjected to mechanical pulverization to achieve a powdered form. The pretreatment procedure involved immersing 30 g of the dried corn cob in one liter of 3N HCl, a solution's temperature was raised to 75 °C and maintained for 5 h. Following this, the mixture experienced reflux in the identical acid at room temperature for 12 h. The treated CC was then rinsed with distilled water for three consecutive, followed by a filtration process. The procedure was repeated three times to ensure the removal of residual acid and was preceded by oven drying at a temperature of 110 °C for 5 h. Subsequently, the pretreated CC was further calcined at a temperature of 700 °C in a muffle furnace, with a constant heat supply rate of 10 °C/min, for 3 h, resulting in the production of nearly white-coloured corn cob ash (CCA).

2.3 Production of Nano Silica from Corncob Ash by Precipitation Method

Silicon dioxide nanoparticles were extracted through a multi-step process. Initially, 20 g of corn cob ash underwent treatment with 150 ml of (3N, 3.5M, and 4N) NaOH, and the resultant mixture underwent refluxing for a duration of 3 h at a temperature of 80 °C. The sodium silicate solution produced was filtered through filter paper by Whatman. The filtrate undergo thorough washing with warm deionized water up to the time it tested alkali-free, determined by the absence of blue colour when tested with pink litmus paper. The process is represented by Equation 1.

$$SiO_2+2NaOH\rightarrow 2NaSiO_3+H_2O \quad (1)$$

The precipitate was transferred to a beaker, and 5N H_2SO_4 was added until the solution became acidic to litmus paper (changing from blue to pink). Equation 2 illustrates the formation of a white gelatinous precipitate.

$$NaSiO_3+H_2SO_4\rightarrow SiO_2+Na_2SO_4+H_2O \quad (2)$$

The resulting precipitate was left on the filter paper for 4 h, washed with deionized water, and finally rinsed with 25 % ammonium hydroxide (NH_4OH) until the

litmus colour shifted from red to blue (indicating a pH of 8). Subsequently, the product was left at room temperature for 4 h, rinsed repeatedly with deionized water until free of alkali, and subsequently subjected to oven drying at 110 °C for 10 h. The obtained powder underwent refluxing with 6N HCl (100 ml) for 4 h, followed by washing with deionized water. Subsequently, 2.5N NaOH (100 ml) was added, stirred, and heated for 3 h at 70 °C. The resulting blend underwent washing with deionized water on a magnetic hot plate with a stirrer. To obtain ccSi nanoparticles, 5N H_2SO_4 was added, followed by washing and filtration with warm deionized water. The nanoparticles were then dried at 110 °C for 12 h in an oven (Figure 1).

Figure 1: Silica nanoparticles produced

2.4 Synthesis of Silica Nanoparticles for Biopolymer Films Reinforcement

Five grams of produced SiNPs were introduced into a beaker containing 100 ml of water (distilled), stirred for five minutes, and then supplemented with 10 g of starch. The resultant mixture underwent stirring for an extra five minutes prior to placement on a hot plate set at 200 °C with continuous stirring for 10mins. Subsequently, 10 g of glycerol was added and stirred for 5 mins. This was subsequently accompanied by the introduction of acetic acid (10 ml), followed by continued stirring for the next 10 mins. The resulting thick slurry mix was then poured and evenly spread on a flat, smooth surface. The blends were subjected to drying at 105 °C in an oven for a period of 2 h, thereafter the films were carefully removed and set aside. This entire procedure was conducted for the *cnSi*, maintaining the same proportion of starch, glycerol and acetic acid. SiNPs are applied in biopolymers for enhanced mechanical properties.

2.5 Characterization of *ccnSi* Extracted

The elemental composition of the extracted *ccnSi* was evaluated with the resource of X-ray fluorescence (XRF) Nitron 3000, while the Brunauer-Emmett-Teller (BET) surface area analyzer, and Malvern Zetasizer dynamic light scattering (DLS) version 7.01 were employed to establish the particles sizes and distribution.

2.6 Characterization of Biopolymer Reinforced with *ccnSi* Particles

The Netherlands-based Phenom-World Eindhoven's Phenom Prox. model of SEM was implemented to evaluate the biopolymer films, while the DSC was applied to examine both the heat needed to raise the temperature and the thermal characteristics of the *ccnSi* particle-reinforced biopolymers. Perkin Elmer TGA4000 (TGA-DTA) was executed to explore the range of decomposition and subsequent reduction and further inspect the process (endothermic or exothermic) of decomposition. Furthermore, Shimadzu FTIR 8400S is used to establish the functional groups in the biopolymer, while the universal testing machine model no UTM-D2 is operated for mechanical testing.

2.7 Optimization

The mixture design method is jointly used with the analysis of variance (ANOVA), response surface plots, and response optimizer are used to achieve multi-response multi-factor optimization of the response model based on the Derringer-modified Harrington's desirability function approach.

3.0 RESULTS AND DISCUSSION

3.1 Characterization of *ccnSi*

3.1.1 SEM-EDX analysis of *ccnSi*

The surface morphology of the *ccnSi* was characterized using SEM-EDX to study the structural form and shape of the particulates. The SEM-EDX spectra in Figure 2 provide information on the percentage composition of the *ccnSi*, while the micrographs provide information on the shapes (texture), nature (crystallinity), and sizes of the *ccnSi* at different alkali concentrations of 3.0, 3.5, and 4.0M NaOH.

The change in colour intensity, shape, and morphology of the *ccnSi* is conspicuous, as the alkali concentration increases, as evident in the transformation from the crystalline phase to the amorphous phase at 4.0M NaOH. This corresponds to the result from FTIR characterization with a disappearance of the band around 3500 cm^{-1} (Figure 3). The images exhibited irregular polygonal shapes and wide particle size range at 3.0 and 3.5M while spherical particles are freely disposed on the surface of the image at 4.0M NaOH with no clear boundaries due to reduced particle size and large agglomeration of particles. The intensity of the image of 4.0M *ccnSi* is lighter owing to lower Si content and higher carbon. A stronger intensity of 3.0 and 3.5M NaOH corresponds to a higher percentage composition of Si and O Peaks in EDX and FTIR. This is in tandem with the particle

size result from DLS and BET analysis confirming a reduction in particle sizes and an increase in porosity as alkali concentration increases.

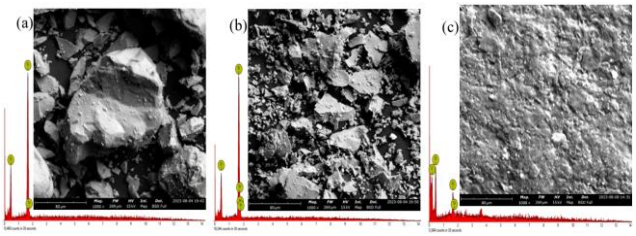

Figure 2: SEM-EDX images of *ccnSi* (a) 3.0 M, (b) 3.5 M, and (c) 4.0 M NaOH treated

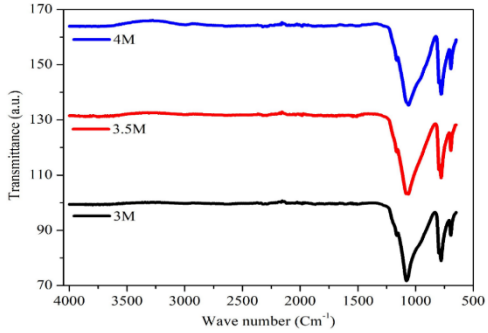

Figure 3: FT-IR Spectra of *ccnSi* of (a) 3.0M (b) 3.5M (c) 4.0M NaOH

3.1.2 FTIR analysis of ccnSi

The molecular, bonding, and functional properties of the as-synthesized *ccnSi* were characterized by FTIR spectroscopy. Silanol and siloxane are well-recognized main chemical groups in silica. Table 1 shows the summary of the peaks while Figure 3 shows the FTIR spectra for the *ccnSi* from corncob at different alkali concentrations. There is a marked absence of silanol groups displaying only absorption peaks for siloxane groups with a slight reduction in intensity as the alkaline concentration increases. Despite minor variations in intensity, the FTIR spectra displayed essentially identical absorption band patterns, as evidenced by the percentage transmittance values. The vibration asymmetry of the siloxane bonds (Si-O-Si) are 1062.2, 1077.2, and 1162.9 cm^{-1}. Similarly, the symmetrical vibration of Si-O-Si theoretical account appears at 779.0 cm^{-1}. Further, the bending vibration of O-Si-O shifted to a higher wave number of 693.2 cm^{-1} (indicating the siloxane bond was forming silicon from silica) for both 3.0M and 3.5M NaOH, a characteristic crystalline cristobalite peak absent in 4.0M NaOH, this agrees with result from SEM images which shows the amorphous nature of 4.0M NaOH. The FTIR result is consistent with the ED-XRF result which shows much lower silica content in 4.0M NaOH, this might account for the loss of peak at 693.2 cm^{-1}, which indicates an incomplete formation of the siloxane group.

Table 1: FTIR absorption peaks wavenumbers for the as-synthesized *ccnSi*

Samples	OH (cm^{-1})	Si-OH (cm^{-1})	Si-O-Si (symmetry) (cm^{-1})	Si-O-Si (asymmetry) (cm^{-1})	O-Si-O (cm^{-1})
3.0M NaOH			779.0	1077.2 1162.9	693.2
3.5M NaOH			779.0	1062.2 1162.9	693.2
4.0M NaOH			779.0	1062.2 1162.9	

Table 2: BET summary of the area-volume analysis of *ccnSi* conducted over many methods

PARAMETERS	3.0M	3.5M	4.0M
Multi-point BET (**surface area, m^2/g**)	324.9	833.6	444.1
DR method micropore volume (**pore vol., cc/g**)	0.1357	0.3286	0.1727
DA method pore diameter (**Pore size, nm**)	2.780	2.920	2.920

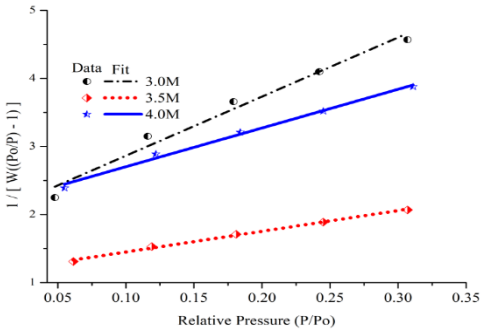

Figure 4: Multipoint BET (a) 3.0M, (b) 3.5 M, and (c) 4.0M *ccnSi* particle

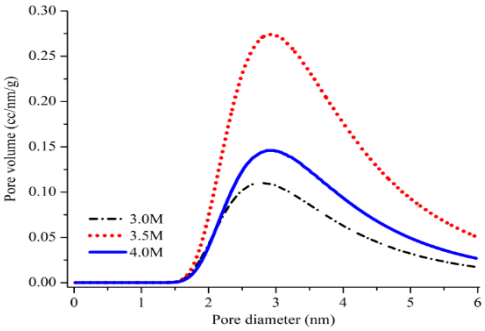

Figure 5: DA of pore volume against pore diameter for (a) 3.0M, (b) 3.5M and (c) 4.0M

3.1.3 BET analysis of *ccnSi*

Quantitative measurements of specific surface area (m^2/g), and the distribution of pore sizes the *ccnSi* was determined using the dynamic Brunauer-Emmet-Teller (BET) multiple point method through gas (nitrogen) adsorption analysis. The result presented in Table 2 shows an increase in surface area (surface energy), pore volume, and pore diameter as the alkali concentration increases from 3.0M to 3.5M, but a reduction was observed at 4.0 M NaOH. The high surface area ranging from 324.9 to 833.6 m^2/g further confirms the as-synthesized *ccnSi* to be in the nano

meter range that is, nanoparticles. Figures 4 and 5 show the multi-point linear relations used to estimate the slope, intercept as well as average surface area (m^2/g) while the DA plots unveil the correlation of pore volume (cc/mm/g) against the pore diameter of which 1.75 nm and 4.75 nm exhibit higher pore volume.

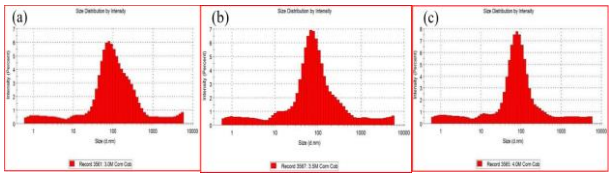

Figure 6: PSD by intensity: (a) 3.0M, (b) 3.5M, and (c) 4.0M NaOH-treated *ccnSi*

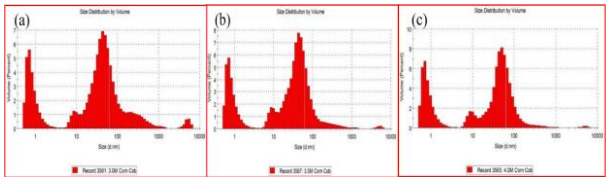

Figure 7: PSD by volume: (a) 3.0M, (b) 3.5M, and (c) 4.0M NaOH-treated *ccnSi*

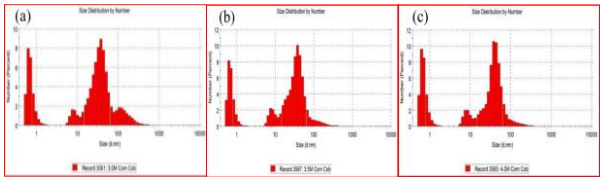

Figure 8: PSD by number: (a) 3.0M, (b) 3.5M, and (c) 4.0M NaOH-treated *ccnSi*

3.1.4 DLS and PSD analysis of ccnSi

The particle size and its distribution were ascertained by DLS, a light scattering-based sizing technique. The intensity-averaged hydrodynamic diameter was calculated from the particle size distribution by intensity, volume, and number (Figures 6-8) and found to decrease as the alkali concentration increased. The poly-dispersity index (PDI), an indicator of the sample's size distribution heterogeneity or agglomeration or aggregation and distribution of molecular mass in a given polymer sample was also calculated. A PDI value exceeding 0.7 suggests a broad size distribution, making the sample likely unsuitable for dynamic light scattering techniques. The International Standard Organization (ISO) has determined that PI values below 0.05 are typical of monodispersed samples, while values above 0.7 are associated with particles having a broad size distribution (standards ISO 2,412:2017 and ISO 22,412:2017) [22]. The particle size (69.23 – 97.70 nm) shown in Table 3 and Figure (6-8) is between 1 to 100nm and hence confirms the nanoparticle nature of the prepared *ccnSi*. The PDI is less than 0.7 which is a pointer that the particle size distribution is not very broad and within detectable limits of DLS. This result corresponds to the surface result from BET as the smaller the particle size, the higher the surface area, and hence 3.5 M NaOH *ccnSi* gives the best result for biopolymer application.

Table 3: Particle size and poly dispersive index of *ccnSi* at varied mole concentration of NaOH

Parameters	3.0 M	3.5 M	4.0 M
Average size (d.nm)	97.70	74.60	69.23
Polydispersity index (PDI)	0.440	0.436	0.463

3.2 Characterization of Biopolymer film

3.2.1 XRF analysis

The elemental composition and purity of the biopolymer films produced from corncobs were analyzed by XRF-FP as presented in Figure 9. The result showed higher *ccnSi* percentages of 94.475 and 94.827 % for 3.0M and 3.5M and a lower percentage of 26.548% for 4.0M biopolymer films, this aligns with the ED-XRF result for the *ccnSi* used for preparing the biopolymer films. However, there is a marginal rise in the quantity of *ccnSi* from 41 % to 44 % for the 3.0M and 3.5M films, and from 10.75 % to 12.41% for the 4.0M film. This confirmed that the biopolymer films contain mainly silica, with an appreciable reduction in metals, alkali-metals, alkaline-earth metals, and their oxides which were the main impurities in the *ccnSi* powder, but present in trace negligible amounts in the biopolymer film. The 3.0M and 3.5M biopolymer films compare favorably and even better than the bioplastic standard utilized in this investigation concerning silica composition.

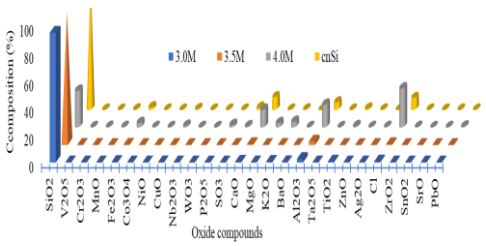

Figure 9: Percentage of oxide composition of *ccnSi* nanoparticles and biopolymer film

3.2.2 SEM analysis

The Scanning electron microscopy (SEM) is used to analyze the surface morphology of the biopolymer film, allowing observation of its shape and structure. The micrographs in Figure 10 provide information on the shapes (texture), nature (crystallinity), and sizes of the biopolymer films and *cnSi* film used for comparison. The 3.0 M film has a nanowire shape, while the 3.5 M film has a spherical shape freely disposed on the surface of the image with a wide

agglomeration of particles and a few nano-ribbons. The 4.0 M film has irregular spherical shape particles with clear boundaries, while the *cnSi* film standard has no clear boundaries as they are largely aggregated and amorphous.

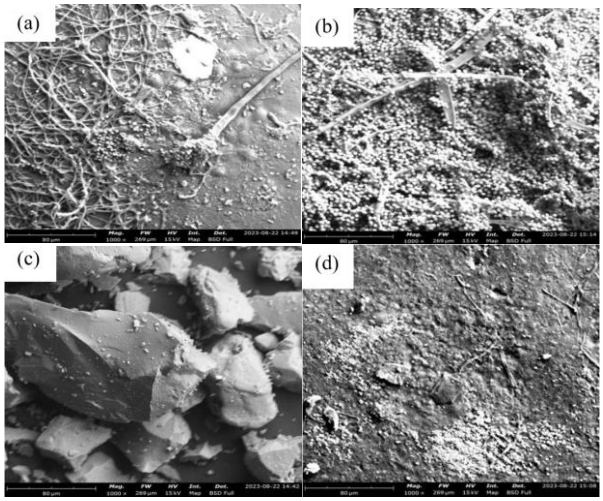

Figure 10: SEM images of biopolymer films with (a) 3.0M (b) 3.5M (c) 4.0M and (d) cnSi standard particles

3.2.3 FTIR analysis

Information about the molecular, bonding and functional properties of the as-synthesized biopolymer films and *cnSi* standard by FTIR spectroscopy is presented in Table 4 and Figure 11. The absorption band of the silanol group in the 3.0M, 3.5M, 4.0M, and the OH bonding in *cnSi* films is characterized by a vibrational absorption band of Si-OH at 1640.0, 1640.0, 1654.9 and 1640.0 cm^{-1}, and abroad band at 3372.6, 3368.8, 3309.8 and 3268.8 cm^{-1} respectively, caused by the water bending molecular vibration confined within the silica matrix. The vibration asymmetry of the siloxane bonds (Si-O-SI) are 1077, 1080, 1073 and 1077 cm^{-1}. The vibrational symmetry of the Si-O-Si framework appears at 760, 852, 682, and 853 cm^{-1}. The 4.0M film showed a slight blue shift in its FTIR absorption bands compared to the other films. The O-Si-O bending vibration at 682.1 cm^{-1} observed for 4.0M is a characteristic of crystalline crystobalite which agrees with the result from SEM images.

Comparing the FTIR results of the biopolymer films with the metasilicate film standards shows that the biopolymer films compare favourably with the commercial metasilicate film standards with closely matched wavenumber values of OH group, Si-OH stretching, O-Si-O bond bending modes, and Si-O-Si asymmetric stretching vibrations.

Table 4: FTIR frequency bands for the biopolymer films and *cnSi* film standard

Reinforced biopolymer films	O-H strand adsorbed water (cm^{-1})	O-H bending (molecular water) (symmetry) (cm^{-1})	Si-O-Si str (asymmetry) in SiO_4 tetrahedron (cm^{-1})	Si-OH bond str (cm^{-1})	OH bending (silanol)
3.0M NaOH	3272.6	1640.0	1077.2	928.1	861.0
3.5M NaOH	3268.8	1640.0	1080.9	928.1	857.2
4.0M NaOH	3309.8	1654	1073.4	943.0	861.0
cnSi film	3268.8	1640.0	1077.2	928.1	853.5

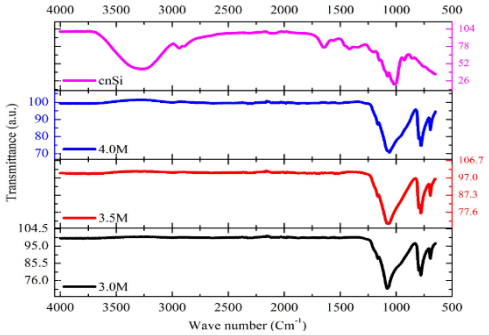

Figure 11: FTIR Spectra for biopolymer films reinforced with 3.0M, 3.5M, 4.0M biopolymer films and *cnSi* particulates

3.2.4 Tensile strength analysis

Tensile strength provides insights into the chemical structure, sample preparation, molecular weight, distribution, crystallinity, and crosslinking of a polymer. The mechanical properties of biopolymer films produced from *ccnSi* from corncob at different alkalis (NaOH) are presented in Figure 12. There was an appreciable decrease in the tensile strength and modulus elasticity but a slight increase in elongation with an increase in alkali concentration from 3.0M to 3.5M. A very high increase in tensile strength from (0.245 to 28.44 MPa) was observed at 4.0M, this may be due to high composition of carbon observed in the ED-XRF spectra of 4.0M film. The increase in the tensile strength also agrees with the FTIR result with several absorption bands representative of bonding and cross-linking. This result showed optimum functionality and strength for biopolymer film at an alkali concentration of 4.0M. The biopolymer film from corncob at 3.0M NaOH treatment with a tensile strength of 0.572 MPa compares favorably with that of the commercial metasilicate of strength 0.49 MPa for its potential use as bioplastic.

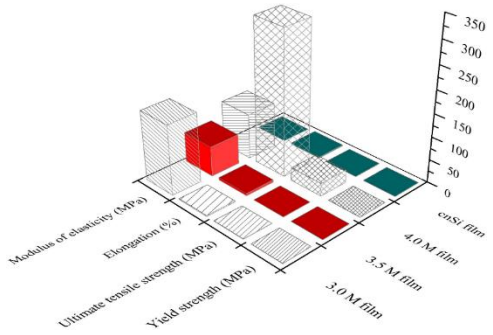

Figure 12: Tensile properties of biopolymer films in comparison with *cnSi* standard

3.2.5 Thermal (TG-DT) analysis

The polymer degradation, thermal stability and its fraction of volatile components by weight change concerning constant heat rate were monitored by TGA. The weight-loss curve shows two distinct losses indicative of the component in the film. Loss above 300 ºC of about 80 % can be ascribed to polymer decomposition. As the ccnSi biopolymer films were heated, thermogravimetric analysis showed the gradual release of adsorbed water and different types of silanol groups from the silica matrix. The inspective TGA-DTA outcomes in thermograms are presented in Figure 13. The differential thermogram exhibits a sharp drop at 100°C, followed by a gentle slope upward to a plateau, a pronounced peak at 350°C, a downward slope to a valley at 470°C, and a final descent to 880°C. The differential thermogram path follows an initial deep well at 100 ºC and then slow growth to a plateau followed by a hillock at 350 ºC and then ash allowed with a minimum at 470 ºC low at the temperature rise to 880 ºC. Thus, *ccnSi* showed two distinct decomposition zones (weight-loss curves) (100–350 ºC and 350– 470 ºC) during heating up to 950 ºC. At around 100-150 ºC the physiosorbed water begins to evaporate. Increasing temperatures lead to the formation of silicic acid, likely due to the disruption of water hydrogen bonds with silanol groups. The sharp transition peak is evidence of the complete removal of trapped or adsorbed water 350 ºC to 470 ºC.

In Figure 13, there was observed weight loss of 2 %, 5 %, 10 %, and 4 % from 3.0M, 3.5M, 4.0M, and *cnSi* films respectively at 300 °C. This arises because of the vaporization of light volatile matter and water. The extrapolated onset temperature (derivative curve) from DTA showing a sharp endothermic peak gives information about the polymer decomposition. 4.0M film gave the least decomposition at 320 °C with a residue of 4 %, 3.0M degraded at 380 °C with a remaining sample weight of 15 %, while the pyrolysis of both 3.5M and *cnSi* film occurred at 400 °C with a remainder weight of 7 % and 17 % respectively. Inflexion points on the curve at 350 °C were observed for 3.0M, 3.5M and *cnSi* films with weight losses of 30 %, 40 %, and 30 % respectively, this is due to condensation of silanol in the high silica films, while 4.0M showed no inflexion point at this temperature.

Thermogravimetry analysis results showed the effect of carbon residues present in 4.0M. This suggests that the *ccnSi*-carbon matrix interfacial bonding is very weak and the maximum degradation temperature is decreased by 80 °C (from 400 to 320 °C) compared to the neat film. This means that the 4.0M film will degrade at a lower temperature and hence less thermally stable. The TGA data demonstrated that the processed *ccnSi* from corncob at 3.0 and 3.5 M NaOH treatment shares the same characteristic properties as the standard amorphous form *cnSi* from Sigma-Aldrich.

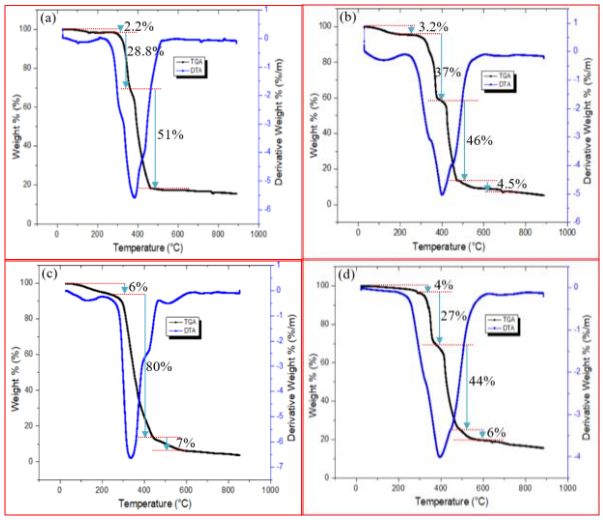

Figure 13: TGA-DTA thermogram of films reinforced with (a) 3.0M (b) 3.5M (c) 4.0M and (d) *cnSi* particulates

3.2.6 Thermal (DSC) analysis

Given the extensive range of polymer formulations developed, thermal analysis can be highly significant in the polymer industry. Thermal analysis identifies the appropriate temperature for making the polymer pliable (easy conversion to film) in an extruder. DSC is a versatile technique that can determine various polymer characteristics, including crystallization, melting, degradation, and phase transitions, as well as T_g, T_c, and T_m. The DSC curves outlined in Figure 14 show the amorphous nature of the biopolymer films and the *cnSi* as the curve shows a glass transition temperature of 32 °C for all the samples, an indication of their poor thermal conductivity and good plastic properties as above this temperature, the polymer behaves like rubber.

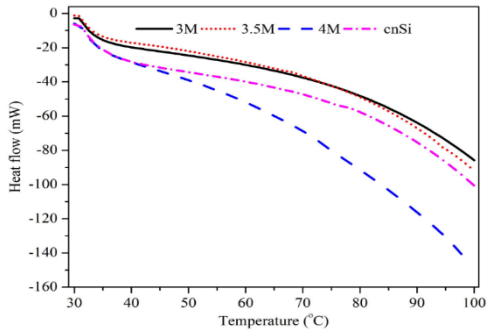

Figure 14: DSC thermograms of films reinforced with 3.0M, 3.5M, 4.0M, and *cnSi* particulates

3.3 Optimization of the Mechanical Response of Biopolymer Film

The composite biopolymer with the highest signal-to-noise ratio is considered the optimal sample. From Table 5, the 4.0M sample with 11.25 g of starch and 3.75 g of *ccnSi* has the optimal tensile strength in terms of signal-to-noise ratio.

Table 5: Shows the experimental design with their experimental results

Sample	Starch (g)	Silica (g)	Glycerol (g)	TENSILE STRENGTH (MPa)	SNRA	MEAN
Control	15	0	10	1.1	0.1069	0.9931
3.5 M	14.375	0.625	9.375	0.25	-0.8633	1.1133
3.0 M	13.75	1.25	10.625	0.82	-0.4148	1.2348
4.0 M	11.25	3.75	10.625	2.85	1.1147	1.7353

3.3.1 Main effect plots for means and signal/noise ratio

The fitting outcomes derived from the Analysis of Variance (ANOVA) were translated into a main effect plot. The main effect plot depicts each parameter's effect at various levels. It was observed that minimum starch and minimum silica give the optimal properties. Figure 15 demonstrates a typical main effect plot of tensile strength which was plotted using the mean of response at each parameter as indicated in Table 5. The maximum tensile strength was found for 11.25 g of starch and 3.75 g of silica, indicating that the best outcomes were achieved with minimal starch and *ccnSi* contents.

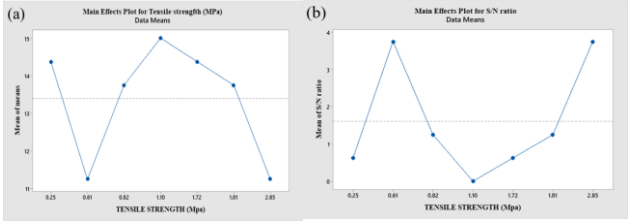

Figure 15: Main effect plots for tensile strength

3.3.2 Response optimization

Response optimizer software was employed to conduct multi-response, multi-factor optimization of response models using the Derringer-modified Harrington's desirability function method. This approach identifies a combination of factor settings that simultaneously optimize multiple responses and determines the optimal settings for addressing a set of multivariate objective functions. As seen in Tables 6 to 7, this optimization is based on the concept of "maximizing the response".

Table 6: Response optimization

Response	Goal	Lower	Target	Importance
Tensile Strength (MPa)	Maximum	0.25	2.85	1

Table 7: Solution of response optimization

Solution	Starch (g)	Silica (g)	Tensile Strength Fit (MPa)	Composite Desirability
1	11.25	3.75	1.73534	0.571286

3.3.3 Response surface plots

Individual and cumulative influences of the factors on the dependent variable as well as mutual interactions between the factors were depicted using response surface plots. The response surface regression equations for tensile strength are written in Equation 3.

$$Tensile\ strength\ (MPa) = 1.358 - 0.371\ (starch) - 0.01\ (starch * ccnSi) \quad (3)$$

The ideal settings of the response and factors are represented in Figure 16 and it can be observed that an increase in silica nanoparticles results in to increase in tensile strength.

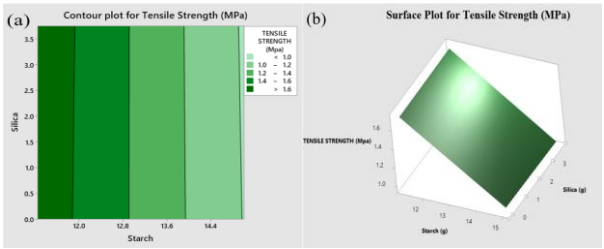

Figure 16: (a) 2D contour and (b) 3D surface plot for varied amounts of starch and nano-silica for tensile strength

4.0 CONCLUSION

Amorphous white *ccnSi* was successfully extracted from corncob, and its suitability for application in bioplastic was investigated. Well-dispersed *ccnSi* particles, with an average size ranging from 69.23 to 97.70 nm, were generated. The extracted *ccnSi*, treated at various alkali concentrations (3.0, 3.5, and 4.0M NaOH), underwent characterization for mechanical, thermal, and barrier properties. Comparisons were made between the *ccnSi* derived from corncob biomass and *cnSi*. XRF and EDX results

confirmed a high silica content of approximately 94%, in contrast to 71.61% found in the *cnSi* standard. SEM revealed that the biopolymer films exhibited significant aggregation and amorphous characteristics, FT-IR confirmed the presence of silanol and silane groups, and BET multiplot displayed a large surface area ranging from 324.9 to 833.6 m^2/g.

The tensile strength of the corncob *ccnSi* film, at 5.83 Kg/cm^2, slightly exceeded the 5.00 Kg/cm^2 of the *cnSi* standard. TGA/DTA demonstrated polymer degradation at 400 ºC, indicating good thermal stability. The glass transition (Tg) value of 32 ºC from DSC further affirmed the amorphous nature of the biopolymer films and the low thermal conductivity, showcasing its potential as a nanofiller for biopolymer-based packaging materials, offering enhanced performance and environmental sustainability. The results indicated favorable comparisons between the *ccnSi* from corncob and *cnSi*, with optimal functionality observed at 3.0M NaOH treatment. This suggests promising potential for the *ccnSi* film as a bioplastic derived from a more economical alternative in agro-waste.

REFERENCES

[1] Ebhota, W. S. and Tabakov, P. Y. "Leveraging agrivoltaics to increase food, energy, and water access in the global south: a case study sub-sarahan Africa", *NIJOTECH*, Vol. 43, no. 2, 2024. https://doi.org/10.4314/NJT.V43I2.20

[2] Tilman, D., Balzer, C., Hill, J. and Befort, B. L. "Global food demand and the intensive nitrogen cycle'. *Proceedings of the National Academy of Sciences*, Vol. 108, no. 50, pp.20260-20264, 2011. https://www.jstor.org/stable/23060109

[3] Gupta, A., Rayeen, F., Mishra, R., Tripathi, M. and Pathak, N. "Nanotechnology applications in sustainable agriculture: An emerging eco-friendly approach" *Plant Nano Biology*, Vol. 4. 100033. 2023. https://doi.org/10.1016/j.plana.2023.100033

[4] Saleem, M. "Possibility of utilizing agriculture biomass as a renewable and sustainable future energy source", *Heliyon*, Vol. 8, no. 2, e08905, 2015. https://doi.org/10.1016/j.heliyon.2022.e08905

[5] Janjua, T. I., Cao, Y., Kleitz, F., Linden, M., Yu, C. and Popat, A. "Silica nanoparticles: A review of their safety and current strategies to overcome biological barriers", *Advanced Drug Delivery Reviews*, Vol. 2203. 115115, 2023. https://doi.org/10.1016/j.addr.2023.115115

[6] Nayl, A. A., Abd-Elhamid, A. I., Ashraf, A. A. and Bräse, S. "Recent progress in the applications of silica-based nanoparticles", *RSC Adv*., Vol. 12, pp.13706-13726. 2022. https://doi.org/10.1039/D2RA01587K

[7] Ragauskas, A. J., Beckham, G. T., Biddy, M. J., Chandra, R., Chen, F., Davis, M. F., Davison, B. H., Dixon, R., Gilna, P., Martin, K., Langan, P., Naskar, A. K., Tschaplinski, T. J., Tuskan, G. A. and Wyman, C. E. "Lignin valorization: Improving lignin process economics through biorefinery development", *Science*, Vol. 344, no.6185, 1246843, 2014. DOI:10.1126/science.1246843

[8] Obi, F. O., Ugwuishiwu, B. O. and Nwakaire, J. N. Agricultural waste concept, generation, utilization and management. *Niger J Technol (NIJOTECH)*, Vol. 35, no. 4, pp.957–964, 2016. https://doi.org/10.4314/njt.v35i4.34

[9] Fangueiro, J. F., de Carvalho, N. M., Antunes, F., Mota, I. F., Pintado, M. E., Madureira, A. R. and Costa, P. S. "Lignin from sugarcane bagasse as a prebiotic additive for poultry feed", *International Journal of Biological Macromolecules*, Vol. 239, 124262, 2023. https://doi.org/10.1016/j.ijbiomac.2023.124262

[10] Baranwal, J., Barse, B., Fais, A., Delogu, G. L. and Kumar, A. "Biopolymer: A Sustainable Material for Food and Medical Applications", *Polymers (Basel)*, Vol. 14, no. 5, pp.983, 2022. doi: 10.3390/polym14050983. PMID: 35267803; PMCID: PMC8912672.

[11] Sadh, P. K., Duhan, S. and Duhan, J. S. "Agro-industrial wastes and their utilization using solid state fermentation: a review", *Bioresour. Bioprocess*, Vol. 5, no. 1, 2018. https://doi.org/10.1186/s40643-017-0187-z

[12] Rhim, J.-W., Park, H.-M. and Ha, C.-S. "Bio-nanocomposites for food packaging applications", *Progress in Polymer Science*, Vol. 38, no. 10–11, pp.1629-1652, 2013. https://doi.org/10.1016/j.progpolymsci.2013.05.008

[13] Olayil, R., Prabu, V. A., DayaPrasad, S., Naresh, K. and Sreekanth, P. S. R. "A review on the application of bio-nanocomposites for food packaging", *Materialstoday: Proceedings*, Vol. 56, Part 3, pp.1302-1306, 2022. https://doi.org/10.1016/j.matpr.2021.11.315.

[14] Sharma, B., Malik, P. and Jain, P. "Biopolymer reinforced nanocomposites: A comprehensive review", *Materialstoday Communications*, Vol. 16, pp.353-363. 2018. https://doi.org/10.1016/j.mtcomm.2018.07.004.

[15] Cazón, P., Velazquez, G., Ramírez, J. A. and Vázquez, M. "Polysaccharide-based films and coatings for food packaging: A review", *Food*

Hydrocolloids, Vol. 68, pp.136-148, 2017. https://doi.org/10.1016/j.foodhyd.2016.09.009.

[16] Wu, Y., Chen, S., Liu, Y., Lu, Z., Song, S., Zhang, Y., Xiong, C. and Dong, L. "One-step preparation of porous aminated-silica nanoparticles and their antibacterial drug delivery applications", *Journal of Materials Science and Technology*, Vol. 50, pp.139-146, 2020. https://doi.org/10.1016/j.jmst.2019.12.015.

[17] Agi, A., Junin, R., Jaafar, M. Z., Mohsin, R., Arsad, A., Gbadamosi, A., Fung, C. K. and Gbonhinbor, J. "Synthesis and application of rice husk silica nanoparticles for chemical enhanced oil recovery", *Journal of Materials Research and Technology*, Vol. 9, no. 6, pp.13054-13066, 2020. https://doi.org/10.1016/j.jmrt.2020.08.112.

[18] Majeed, K., Ahmed, A., Abu Bakar, M. S., Indra Mahlia, T. M., Saba, N., Hassan, A., Jawaid, M., Hussain, M., Iqbal, J. and Ali, Z. "Mechanical and Thermal Properties of Montmorillonite-Reinforced Polypropylene/ Rice Husk Hybrid Nanocomposites", *Polymers*, Vol. 11, no. 10, 1557, 2019. https://doi.org/10.3390/polym11101557

[19] Hoidy, W., Mansor, A., Emad, A. and Nor, I. "Preparation and Characterization of Polylactic Acid/Polycaprolactone Clay Nanocomposites", *Journal of Applied Sciences*, Vol. 10, no. 2, pp.97-106. 2010. DOI: 10.3923/jas.2010.97.106.

[20] Ferraz, D. and Pyka, A. "Circular economy, bioeconomy, and sustainable development goals: a systematic literature review", *Environmental Science and Pollution Research*, Vol. 11, no. 10, 2023. https://doi.org/10.1007/s11356-023-29632-0

[21] Ellen MacArthur Foundation. "The Circular Economy in Detail", 2017. Retrieved from https://www.ellenmacarthurfoundation.org/

[22] Mujtaba, M., Morsi, E., Kerch, G., Elsabee, Z., Kaya, M., Labidi, J. and Khawar M. Current advancements in chitosan-based film production for food technology; A review. Int. J. Biol. Macromol. 2019;121: 889-904.